

ELEVENTH EUROPEAN ROTORCRAFT FORUM

Paper No. 84

A REVIEW OF THE APPLICATIONS OF A HORIZONTAL TAIL IN THE
SINGLE MAIN AND TAILROTOR HELICOPTER

A.E. Caldwell, S.S. Houston, D.G. Thomson,
Department of Aeronautics, University of Glasgow.

September 10-13, 1985
London, England.

THE CITY UNIVERSITY, LONDON, EC1V 0HB, ENGLAND.

A REVIEW OF THE APPLICATIONS OF A HORIZONTAL TAIL IN THE SINGLE MAIN AND TAILROTOR HELICOPTER

A.E. Caldwell, S.S. Houston*, D.G. Thomson,
Department of Aeronautics, University of Glasgow.

Abstract

A current preoccupation of the designers of fixed-wing aircraft is the extent to which ACT might allow a reduction in tailplane size with a consequent reduction in trim drag. The role of ACT would be to compensate for the loss of stability caused by bringing the c.g. aft in order to reduce the severity of the trim requirement. The same does not apply to helicopters because they can be trimmed without a tailplane. They could dispense with the tailplane altogether and rely on feedback control to the main rotor to restore stability where necessary. There would, however, be no obvious performance benefits in doing this, and it would deprive the helicopter of the tailplane's other important function, which is to adjust the fuselage attitude.

The paper enlarges on the issues presented above. The longitudinal stability and control of fixed-wing aircraft is compared and contrasted with that of helicopters, and the impact of ACT on the sizing of the horizontal tail discussed. The results of computer studies of a decoupled flight path/attitude control system for a helicopter are presented, from which it is argued that, in contrast to fixed-wing aircraft, helicopters might benefit from harnessing ACT to larger rather than smaller tailplanes than are currently employed.

1. Introduction

The majority of both fixed-wing aircraft and helicopters have tailplanes. The two groups differ, however, in that fixed-wing aircraft cannot fly without them (or without some device to take the place of the tailplane) whereas helicopters, on the whole, can, although their handling qualities may leave something to be desired.

The tailplane of a fixed-wing aircraft is essential to enable the aircraft to be trimmed, that is, to achieve equilibrium in steady flight. It also influences the stability of the aircraft by supplying both damping in pitch and a small measure of static stability with respect to incidence, but these functions are of lesser importance, particularly the second, which can be fulfilled more effectively by the main wing provided that the c.g. is far enough forward. It is the forward c.g. which establishes the severity of the trim requirement and therefore the size of the tailplane. "Reduced static stability" allied to active control technology (ACT) offers improved performance through a reduction in tailplane size. The idea is to bring the c.g. further aft than would normally be acceptable in order to lessen the trim force required of the tailplane, and to compensate for the reduction in static stability by applying feedback control to the elevator. It is not just that a certain amount of structural weight is saved. The trim force generated by the tailplane is downwards and so the main wing has to generate more lift than would otherwise be

* Now Flight Research Division, Royal Aircraft Establishment, Bedford.

necessary. The extra induced drag entailed by this process, combined with the induced drag attributable to the lift required to support the weight of the tailplane and the induced drag generated by the tailplane itself, is known collectively as trim drag, and it is mainly through a reduction in trim drag that performance benefits can be realised.

The role which the location of the c.g. plays with regard to the stability and control of fixed-wing aircraft has no counterpart in helicopters. It is not too much of an oversimplification to imagine the fuselage of the helicopter pendulously supported underneath the main rotor, so that the c.g. location merely affects the fuselage attitude without influencing the dynamics of the system. The helicopter does not therefore need its tailplane to achieve equilibrium in steady flight and in this respect the tailplane requirement is fundamentally different from that of fixed-wing aircraft. In other respects it is the same: the tailplane supplies pitch damping and static stability with respect to incidence, of which the second is rather more important than in the fixed wing case since the main rotor is unstable with respect to incidence.

There are no obvious performance gains to be made by applying ACT to the helicopter tailplane. There are, however, other potential benefits associated with the opportunity to control the fuselage attitude independently of the flight path. These are explored in sections 4 to 6 below. Before that, in sections 2 and 3, some basic flight mechanics is presented, with the fixed-wing case included for comparison.

2. Fixed-Wing Aircraft Logitudinal Stability and Control

The following is intended to provide a brief reminder of some aspects of fixed-wing aircraft longitudinal stability and control, with particular reference to the tailplane function.

Fig. 1 shows an aircraft in level flight. The equation to be satisfied for pitch equilibrium, obtained by taking moments about the c.g. is,

$$M = M_{wb} - L_{wb} \bar{c} (h_{wb} - h) - L_t l_t = 0 \quad - (1)$$

(Standard notation is used throughout this section and so the symbols will not be defined in the text. A comprehensive list of notation is given at the end).

The influence of the static margin can be made explicit as follows. Firstly, the length l_t is replaced with the expression $(l_t' + (h_{wb} - h)\bar{c})$ in order to show the dependence on c.g. position and then the expression for M is non-dimensionalised by dividing by $1/2 \rho V^2 S \bar{c}$ to give

$$\begin{aligned} C_M &= C_{M_{wb}} - C_{L_{wb}} (h_{wb} - h) - V_H' C_{L_t} - (h_{wb} - h) \frac{S_t}{S} C_{L_t} \\ &= C_{M_{wb}} - C_L (h_{wb} - h) - V_H' C_{L_t} \end{aligned} \quad - (2)$$

The neutral point is the c.g. location (value of h) such that $dC_M/d\alpha$ is zero, i.e.

$$0 = \frac{dC_L}{d\alpha} (h_{wb} - h_n) - V_H' \frac{dC_{L_t}}{d\alpha_t} \frac{d\alpha_t}{d\alpha}$$

$$\Rightarrow h_{wb} = h_n - V_H' \frac{a_t}{a} \left(1 - \frac{d\epsilon}{d\alpha}\right) \quad - (3)$$

Due to the influence of the tail, the neutral point is behind the aerodynamic centre of the wings and fuselage alone. In terms of h_n , the expression for the pitching moment coefficient about the c.g., equation (2), becomes

$$\begin{aligned} C_M &= C_{M_{wb}} - C_L (h_n - h) + V_H' \left[C_L \frac{a_t}{a} \left(1 - \frac{d\epsilon}{d\alpha}\right) - C_{L_t} \right] \\ &= C_{M_{wb}} - C_L K_n + V_H' \left[C_L \frac{a_t}{a} \left(1 - \frac{d\epsilon}{d\alpha}\right) - C_{L_t} \right] \end{aligned} \quad - (4)$$

To trim ($C_M = 0$), the tail volume ratio V_H' has to increase with increasing static margin K_n . Assuming that the moment arm l_t' is fixed by other considerations, this means that more tail surface area is required as the design static margin gets bigger.

The actual size of the tailplane will usually be such as to provide a sufficiently large value of $[V_H' (-C_{L_t})_{\max}]$ to achieve some critical condition of longitudinal manoeuvring flight. This results in an equation similar to (4). For example, referring to Fig. 2, the condition for rotation at take-off is obtained by setting to zero the resultant moment about the rear undercarriage position, i.e.

$$0 = M_{wb} + L_{wb} \bar{c} (h_u - h_{wb}) - mg \bar{c} (h_u - h) - L_t [l_t' + (h_{wb} - h_u) \bar{c}]$$

In coefficient form, with $C_w = (1+\delta)C_L$, and making use of (3), the above equation becomes

$$0 = C_{M_{wb}} - C_L K_n - C_L \delta (h_u - h) + V_H' \left[C_L \frac{a_t}{a} \left(1 - \frac{d\epsilon}{d\alpha}\right) - C_{L_t} \right] \quad - (5)$$

The importance of the undercarriage location is clearly seen in equation (5) in the term $-C_L \delta (h_u - h)$, but the static margin still exerts a strong influence.

Thus the amount of tailplane area required can be reduced by decreasing the static margin. From the point of view of achieving a given trim state, the area can be made arbitrarily small by judicious placement of the c.g. and the landing gear with respect to the neutral point, but of course a certain amount of tail surface area will be required to maintain pitch control throughout the flight envelope. As the static margin becomes large and negative the size of the tailplane has to increase again to maintain trim, although there is the advantage that the tailplane is now operating at positive C_{L_t} thereby assisting the main wing and reducing the trim drag. The optimum is probably small negative K_n .

The degradation in inherent stability caused by reducing K_n and, by implication, S_t , is quite severe. The primary effect of having a positive static margin is that following a disturbance in pitch, the

couple formed by the incremental lift acting through the neutral point and the equal and opposite incremental inertia force acting through the c.g. is such as to counteract the disturbance. K_n feeds through into a flight dynamics analysis as the dominant part of the "spring stiffness" term in the short period oscillation. S_t affects the pitch damping of the aircraft and therefore the damping of the short period oscillation.

Fig. 3 shows the effect of decreasing tailplane size on the longitudinal stability characteristics of the hypothetical aircraft whose leading data and linearised equations of motion are given in Table 1. The aircraft is based on the worked example in Chapter 13 of ref. 1. The term $(0.495 + 0.725V_H')$ which appears in a number of aerodynamic derivatives is simply l_t/l_t' the moment arm l_t' being fixed so that S_t is directly proportional to V_H' . In deriving the expressions for the aerodynamic derivatives, it has been assumed that the static margin decreases with tailplane size in order to satisfy the critical trim criterion according to the following relationship (c.f. equations (4) and (5))

$$K_n = -1.162 + 1.955V_H' \quad - (6)$$

At the design point ($V_H' = 0.63$), the aircraft exhibits classical stability characteristics as shown in Table 4. It becomes unstable at $V_H' = 0.594$ (6% reduction in S_t), but quite a lot happens before that: the short period and phugoid oscillation break up into four aperiodic modes of which two combine to give an entirely new oscillatory mode. (This kind of behaviour has also been reported by Etkin, ref. 2). The main point is that a very modest reduction in tailplane size causes a stable aeroplane with acceptable handling qualities to become unstable. Therefore, to reap the performance benefits associated with reduced tailplane size, the control strategy has to change fundamentally, from traditional open loop control to full authority automatic control.

3. Helicopter Longitudinal Stability and Control

The situation with regard to helicopters is somewhat different as can be seen from Figs. 4 and 5 which have been plotted using data derived from the programme HELISTAB (ref. 3) developed at the Royal Aircraft Establishment, Bedford. Two different helicopter types are represented, the first being a rigid rotor helicopter in the 4000 kg class, broadly similar to the Westland Lynx, and the second an articulated rotor helicopter weighing 5500 kg, broadly similar to the Aerospatiale Puma. Leading data are contained in Tables 2 and 3.

Since the tailplane is not required to trim the aircraft, its size can be reduced for the purposes of investigating dynamic stability without the need to make other compensatory changes, and can be taken right down to zero. The effect on the rigid rotor helicopter is to make an already unstable vehicle more unstable, but not drastically so until the tailplane is diminished to half the standard size, at which point the low modulus phugoid-type mode becomes aperiodic. The articulated rotor helicopter is stable at the design point (Table 4). The low modulus oscillatory mode becomes unstable with about 70% of the original tailplane area, but does not degenerate

into aperiodic modes until the tailplane is removed altogether. If the tailplane size is trebled, the rigid rotor helicopter just becomes stable, while the effect on the articulated rotor vehicle is minimal.

It would not appear to be such a radical departure from current practice to have helicopters without tailplanes. In a large number of cases they are unstable over part of the flight envelope in any case and are fitted with electrical feedback systems to render them stable. It may be that the reliability and authority of such feedback systems would have to be increased for particular aircraft in the event that they became unflyable minus both tailplane and SAS, but the basic principle of using feedback control to confer stability is already established.

There are, however, good reasons for retaining the tailplane even although the technology exists to dispense with its services in relation to dynamic stability. The tailplane on a helicopter is used to trim the fuselage attitude, and in some cases the size of the tailplane is determined by the need to establish a particular attitude at a particular flight condition (ref. 4) rather than from considerations of dynamic stability. The dynamic equilibrium of steady flight depends primarily on the rotor operating state and its attitude with respect to the aircraft's velocity vector: the fuselage finds its own attitude relative to the rotor such that the sum of the moments about the c.g. due to the forces and moments produced by the rotor at the hub, and to the fuselage aerodynamic loading, is zero. This balance, and therefore the fuselage attitude relative to the rotor in a given flight condition, can be affected by a tailplane (taken to be part of the fuselage). There are several reasons why it might be desirable to adjust the fuselage attitude in this way, of which two stand out as being of particular importance. The first is that control margins can be changed. If the fuselage changes its attitude with respect to the rotor whilst the same condition of steady flight is maintained, then the fuselage attitude changes by the same amount relative to the swashplate (or whatever device controls blade cyclic pitch) since the swashplate must hold its attitude in relation to the rotor or else the rotor operating state changes. The cockpit inceptors control the attitude of the swashplate relative to the fuselage and so their positions change. The second is that the amplitude of blade flapping changes, and with it the amplitude of the n per rev. (n = number of blades) hub moment which has a major effect on the fatigue life of the rotor head. This consideration is especially important for helicopters having rotors of high flapping stiffness which have the capacity to generate large hub moments.

Other possible reasons for adjusting the fuselage attitude are to optimise visibility, to improve ride comfort, to minimise drag and to assist weapons aiming. In teetering rotor helicopters, large excursions in fuselage attitude are possible in conditions of low rotor thrust and so a measure of tailplane control is important.

4. ACT Applied to Tailplanes

When considering fixed-wing aircraft, it seems fairly clear that the most significant advantage conferred by ACT lies in the possibility of reducing the tailplane size. Design studies to quantify the performance benefits that might be attainable have been

carried out. For example, Kurzhals (ref. 5) quotes a 9% reduction in drag for a combat aircraft in which the tailplane area is decreased by 35% from that of the baseline configuration, while Hitch (ref. 6) indicates that for civil aircraft, a more modest reduction in area of 20% would reduce direct operating costs by something like 1.5% without too severe a degradation in inherent stability. Given that helicopters have small tailplanes in comparison with fixed-wing aircraft (Tables 5 and 6), and that the flight control function is not the only one, perhaps not even the main one, to be fulfilled by the tailplane, there is no clear advantage in eliminating it and using ACT applied to the main rotor to correct the resulting handling deficiencies in spite of the fact that it would be a relatively small step to take.

On the contrary, in view of the importance of fuselage trimming, there would appear to be a strong case for enlarging the size of the tailplane and using ACT to provide decoupled flight path/attitude control. This would go beyond the present level of tailplane control technology, which operates with manual trimmers or with slow-acting automatic trimmers independent of the primary flight control system. The aim would be to have the tailplane control fully integrated with the primary flight controls such that the pilot could command fuselage pitch attitude (to a limited extent) independently of the flight path. It is envisaged that the principal use of decoupled attitude control would be to acquire and track targets; secondary uses could include any of those listed at the end of section 3. Although helicopter armaments are increasingly of the type which do not require the aircraft to point at its target, the extent of the permitted misalignment is still limited, and so the performance of the vehicle/weapon system would be improved by releasing the pitch degree of freedom. There is a varied literature which deals with the desirability of fuselage pointing of which refs. 7, 8 and 9 in particular mention helicopter vs. helicopter air combat. To date the emphasis has been on lateral pointing, by sideslipping, presumably because of the difficulty of decoupling the pitch attitude from the flight path.

There have been comparable developments in the fixed-wing field, most notably in the AFTI (Advanced Fighter Technology Integrator) programme, in which an F-16 has been equipped with additional control surfaces to allow fuselage pointing, with demonstrable advantages in target acquisition and tracking (ref. 10). This is counter to the general trend for fixed wing aircraft. Helicopters, however, are uniquely suited to exploit this type of agility, having already direct lift control and a high level of decoupled yaw attitude control.

5. A System for Decoupled Attitude Control

The control system was designed in connection with the simulation of a target tracking manoeuvre. The equations used to represent the helicopter were of the linearised derivative type, based on the rigid rotor configuration of Table 2. It was assumed that the minimum speed at which decoupled attitude control might be required was 80 knots, this being roughly the minimum power speed of the chosen configuration and possibly representative of future NOE ("nap of the earth") speeds. The tailplane area had to be trebled to enable it to pitch

the helicopter by $\pm 5^\circ$ at this speed without stalling. This immediately highlights one of the fundamental problems, namely the large increase in S_t required to provide a modest amount of pitch attitude control. The problem is particularly severe for the configuration selected for this exercise. Helicopters with articulated rotors might be expected to achieve similar performance with a less dramatic increase in tailplane size, but the difficulty remains that for certain types the weight penalty may be too great.

A schematic representation of the flight control system is shown in Fig. 6. The precompensator, feedback and feed forward matrices were each derived in separate steps, reflecting to some extent the evolution in the requirements of the FCS as the study progressed. A better overall design might possibly have been accomplished in a single step using the techniques of modern control theory, but the method used here resulted in an FCS which enabled the simulation to be carried out satisfactorily without the need to go through the design process again.

For the purposes of carrying out the mathematical procedures involved in the design, the system dynamics were represented in the conventional state space format

$$\dot{\underline{x}} = \underline{A} \underline{x} + \underline{B} \underline{u} \quad - (7)$$

in which the system matrix \underline{A} and control matrix \underline{B} were functions of the trim state. The state vector \underline{x} contained perturbation states ordered $(u, w, q, \theta, v, p, \phi, r, \psi)$. As a first step, the first two of these, which are all body axis components, were replaced with the earth axis components ΔV_f and γ using the relationships

$$\left. \begin{aligned} u &= \Delta V_f \cos \theta_e + \gamma V_{fe} \sin \theta_e - \theta V_{fe} \sin \theta_e \\ w &= \Delta V_f \sin \theta_e - \gamma V_{fe} \cos \theta_e + \theta V_{fe} \cos \theta_e \end{aligned} \right\} \quad - (8)$$

and the system and control matrices were correspondingly modified. The purpose of doing this was to make explicit the variables that had to be controlled.

The precompensator matrix provided cross-feeds between the controls such that a single inceptor movement forced only the desired degree(s) of freedom. Mathematically, this amounts to a transformation of the control vector \underline{u} and control matrix \underline{B} as follows:

$$\left. \begin{aligned} \underline{u} &= \underline{K}_p \underline{u}_p \\ \underline{B} \underline{u} &= \underline{B} \underline{K}_p \underline{u}_p = \underline{B}_p \underline{u}_p \end{aligned} \right\} \quad - (9)$$

The control vector is of length 5 to incorporate the tailplane setting angle, the order being $(\theta_0, \theta_{1s}, \theta_{1c}, \theta_{otr}, \alpha_s)$, and \underline{K}_p is the 5 x 5 precompensator matrix.

The desired structure for \underline{B}_p was

$$\begin{array}{c}
 \Delta V \\
 \gamma \\
 q \\
 \theta \\
 v \\
 p \\
 \phi \\
 r \\
 \dot{v}
 \end{array}
 \begin{bmatrix}
 u_{p_1} & u_{p_2} & u_{p_3} & u_{p_4} & u_{p_5} \\
 0 & 1 & 0 & 0 & 0 \\
 1 & 0 & 0 & 0 & 0 \\
 0 & 0 & 0 & 0 & 1 \\
 0 & 0 & 0 & 0 & 0 \\
 0 & 0 & 0 & 1 & 0 \\
 0 & 0 & 1 & 0 & 0 \\
 0 & 0 & 0 & 0 & 0 \\
 0 & 0 & 0 & 0 & 0 \\
 0 & 0 & 0 & 0 & 0
 \end{bmatrix}$$

where the elements denoted '1' were to be as close to their counterparts in \underline{B} as possible and those denoted '0' were to be as small as possible. The thinking behind this was to reduce cross-coupling whilst retaining the primary control characteristics. Taking the inceptors for the controls u_{p_j} to be the same as those for u_j in the uncompensated system, it can be seen from the structure of \underline{B}_p that collective, longitudinal cyclic, tailplane and lateral cyclic were to control respectively flight path angle, speed, pitch rate and roll rate. No attempt was made to decouple sideslip and yaw.

\underline{K}_p was obtained as the solution to the following least squares problem:

minimise $g(K_{p_{ij}})$ with respect to all $K_{p_{ij}}$

$$\begin{aligned}
 \text{where } g = & B_{p_{11}}^2 + (B_{p_{12}} - B_{12})^2 + \dots + B_{p_{15}}^2 \\
 & + (B_{p_{21}} - B_{21})^2 + \dots + B_{p_{25}}^2 \\
 & + \\
 & + \text{etc}
 \end{aligned}
 \tag{10}$$

$$\text{and } B_{p_{ij}} = B_{ik} K_{pkj}$$

Table 7 shows the \underline{B} and \underline{B}_p matrices at 60 and 160 knots, from which it is apparent that this ploy has been fairly successful, the pitch and roll rates (rows 3 and 6) being dominated each by a single controller. It was found to be impractical to isolate the speed degree of freedom from the climb controller at speeds above 120 knots, and so above this speed the structure of the \underline{B}_p matrix was changed such that the schematic representation composed of '1's and '0's would have a '1' in the top left hand corner. The results shown in Table 7 incorporate this modification.

The purpose of the feedback matrix was to reduce the inherent coupling between the states implicit in the system matrix \underline{A} and to minimise the effect of external disturbances on the system. It was calculated on the basis of optimal control theory (ref. 11), by minimisation of the quadratic performance index

$$J = 1/2 \int_0^{\infty} (\underline{x}^T \underline{Q} \underline{x} + \underline{u}^T \underline{R} \underline{u}) dt \tag{11}$$

where \underline{Q} and \underline{R} are diagonal weighting matrices which penalise excursions in the state and control variables respectively. The theory shows that the optimal feedback strategy

$$\underline{u}_{pf} = \underline{K} \underline{x} \quad - (12)$$

is such that \underline{K} is given by

$$\underline{K} = \underline{R}^{-1} \underline{B}^T \underline{M} \quad - (13)$$

where \underline{M} is the solution of the matrix-Riccati equation

$$\underline{M} \underline{A} - \underline{M} \underline{B} \underline{R}^{-1} \underline{B}^T \underline{M} + \underline{Q} + \underline{A}^T \underline{M} = \underline{0} \quad - (14)$$

This equation was solved using the Potter algorithm (ref. 12).

Initial values for the elements of \underline{Q} and \underline{R} were determined (ref. 13) by the relationship

$$Q_{ii} = \frac{1}{x_{i2}^2_{\max}}, \quad R_{ii} = \frac{1}{u_{i2}^2_{\max}} \quad - (15)$$

Improved values emerged from a large number of numerical experiments in which the effects of varying the Q_{ii} and R_{ii} one at a time on the system dynamics were systematically investigated. Tables 8-11 show some of the response characteristics of the resulting closed loop system at 100 knots. The time taken by the system to recover from a disturbance in forward speed is fairly large (4.76 seconds to 5% of the initial value), but disturbances in flight path angle and pitch attitude are damped out much more quickly. In general, the level of coupling between the states is low.

The feedforward matrix simply scales the inceptor outputs in relation to certain desired steady states. The system equations can be represented in the following way

$$\dot{\underline{x}} = (\underline{A} - \underline{B}_p \underline{K}) \underline{x} + \underline{B}_p \underline{u}_{pd} \quad - (16)$$

where \underline{u}_{pd} is the control action demanded by the pilot. Steady state solutions are those given by the above equation with $\dot{\underline{x}}$, \dot{p} , \dot{q} and \dot{r} all zero. The state vector can be reduced to $\underline{x}_R = (\Delta V_f, \gamma, \theta, v, \phi, \psi)$. The equations corresponding to θ , ϕ and ψ are all identically satisfied and so the steady state solutions are those satisfying the following system of six equations:

$$(\underline{A} - \underline{B}_p \underline{K})_R \underline{x}_R + \underline{B}_{pR} \underline{u}_{pd} = \underline{0} \quad - (17)$$

Clearly an arbitrary \underline{x}_R cannot be generated since there are six states and only five controls (mathematically, \underline{B}_{pR} is 6x5 and cannot be inverted) but a longitudinal subset of three states ($\Delta V_f, \gamma, \theta$) and three controls (u_{p1}, u_{p2}, u_{p5}) does allow a general solution in the form

$$\begin{bmatrix} u_{p1} \\ u_{p2} \\ u_{p5} \end{bmatrix} = \begin{bmatrix} \underline{K}_{FR} \end{bmatrix} \begin{bmatrix} \Delta V_{fd} \\ \gamma_d \\ \theta_d \end{bmatrix} \quad - (18)$$

where K_{FR} is the reduced feedforward matrix and the suffix d has been added to the states to indicate that these are demanded steady states. The full feedforward matrix is obtained by augmenting the system of equations to

$$\begin{bmatrix} u_{p_1} \\ u_{p_2} \\ u_{p_3} \\ u_{p_4} \\ u_{p_5} \end{bmatrix} = \begin{bmatrix} K_{FR_{11}} & K_{FR_{12}} & 0 & 0 & K_{FR_{13}} \\ K_{FR_{21}} & K_{FR_{22}} & 0 & 0 & K_{FR_{23}} \\ 0 & 0 & 1 & 0 & 0 \\ 0 & 0 & 0 & 1 & 0 \\ K_{FR_{31}} & K_{FR_{32}} & 0 & 0 & K_{FR_{33}} \end{bmatrix} \begin{bmatrix} \Delta V_{fd} \\ \gamma_d \\ u_{p_3} \\ u_{p_4} \\ \theta_d \end{bmatrix} \quad - (19)$$

The emphasis was placed on controlling the longitudinal states because of the requirements of the tracking manoeuvre which was to be simulated. The demanded states (ΔV_{fd} , γ_d , θ_d) are not obtained exactly because of residual cross-coupling between the lateral and longitudinal dynamics: in other words equations (18) are not strictly compatible with equations (17).

Further details of the techniques described in this section are contained in ref. 14.

6. Simulation of a Target Tracking Manoeuvre

The simulation was carried out in the context of helicopter vs helicopter air combat. It was assumed that the target was flying 50 m above the helicopter on a reciprocal track at 150 knots, and that it was 1000 m away when the manoeuvre was started. The helicopter was trimmed in level flight at 100 knots and was required to sustain this flight state whilst tracking the target for as long as possible, the target being off limits when the pitch attitude demanded of the helicopter either caused the tailplane to stall (at 15° angle of attack) or produced a hub moment in excess of 35 kN-m.

The commanded pitch attitude was given by

$$\theta_d = \arctan \left[\frac{50 - z_e}{1000 - x_e - V_{ftgt}} \right]$$

where z_e and x_e were measured from the start of the manoeuvre. The dynamics of the θ_d calculation were not included in the simulation, but this omission was partially offset by requiring the helicopter to point directly at the target, which is a little severe.

The results of the simulation are presented in figs. 7-10. Fig. 7 shows the pitch attitude perturbations necessary to perform the manoeuvre, from which it is seen that the target was acquired in less than one second and thereafter tracked accurately. The demanded flight path was held within tight limits as shown in Figs. 8 and 9. Fig. 10 shows the control activity (actuators, not inceptors).

The manoeuvre ended after 4.25 seconds when the pitch attitude perturbation reached 6.5°, at which point the tailplane stalled. The trim pitch attitude had been set to give zero hub moment but in spite of this the hub moment reached 30 kNm towards the end of the manoeuvre, which is close to the limiting value of 35 kNm.

7. Conclusions.

- The arguments for using ACT to reduce the size of the tailplane on fixed-wing aircraft do not apply to helicopters.

- It would be feasible to eliminate the tailplane from helicopters and use conventional SAS to correct handling deficiencies.

- Not only are there no obvious performance gains to be made by eliminating the tailplane from helicopters, but such a step would remove the capability to adjust the fuselage attitude.

- By making the helicopter tailplane accessible to the primary flight control system and using ACT, new flight modes are made possible, such as fuselage pointing without speed or flight path deviations.

- To take advantage of the increased agility which could be made available, certain helicopters, notably those with stiff flapwise rotors, will require larger tailplanes than they currently possess.

- The potential gains in agility will have to be weighed against the increased weight and complexity of the vehicle.

- The impact of ACT on helicopters may be to produce larger rather than smaller tailplanes.

References

- 1) A.W. Babister, Aircraft Dynamic Stability and Response, Pergamon Press, 1980.
- 2) B. Etkin, Dynamics of Flight - Stability and Control, John Wiley, 1982.
- 3) G.D. Padfield, A Theoretical Model of Helicopter Flight Mechanics for Application to Piloted Simulation, R.A.E. TR 81048, 1981.
- 4) B.B. Blake and I.B. Alansky, Stability and Control of the YUH-61A, Paper presented at the 31st Annual National AHS Forum, 1975.
- 5) P.R. Kurzhals, Systems Implications of Active Controls, AGARD-CP-260, 1979.
- 6) H.P.Y. Hitch, Active Controls for Civil Aircraft, The Aeronautical Journal of the Royal Aeronautical Society, Vol. 83, No. 826, Oct. 1979.
- 7) W. Steward, Operational Criteria for the Handling Qualities of Combat Helicopters, AGARD-CP-333, 1982.
- 8) M.V. Lowson and D.E.H. Balmford, Future Advanced Technology Rotorcraft, The Aeronautical Journal of the Royal Aeronautical Society, Vol.84, No. 830, Feb. 1980.
- 9) H.C. Curtiss, Jr. and G. Price, Studies of Rotorcraft Agility and Manoeuvrability, Paper presented at the 10th European Rotorcraft Forum, 1984.
- 10) Col. D.W. Milan and F.R. Swortzel, Automating Tactical Fighter Combat, Aerospace America, Vol.22, No.5, May, 1984.
- 11) R.J. Richards, An Introduction to Dynamics and Control, Longman, 1979.
- 12) J.E. Potter, Matrix Quadratic Solutions, J. Siam Applic. Math., Vol. 14, No. 3, 1966.
- 13) P.M. Brodie, Use of Advanced Control Theory as a Design Tool for Vehicle Guidance and Control, AGARD-CP-137, 1974.
- 14) S.S. Houston, On the Benefit of an Active Horizontal Tailplane to the Single Main and Tailrotor Helicopter, Ph.D. Thesis, Glasgow University, 1984.
- 15) R.K. Heffley et al., A Compilation and Analysis of Helicopter Handling Qualities Data, NASA Contractor Report 3144, 1979.
- 16) J.W.R. Taylor (Editor), Jane's All The World's Aircraft, Jane's Publishing Co. Ltd., 1984.

Notation

\underline{A}	System matrix
\underline{A}^T	Transpose of system matrix
a	Lift curve slope
a_b	Lift curve slope of tailplane
\underline{B}	Control matrix
\underline{B}_p	Precompensated control matrix
\underline{B}^T	Transpose of control matrix
C_L	Aircraft lift coefficient
C_{L_t}	Tailplane lift coefficient
$C_{L_{wb}}$	Lift coefficient of wing-body combination (aircraft less tail)
C_M	Pitching moment coefficient about c.g.
$C_{M_{wb}}$	Pitching moment coefficient of wing-body combination (aircraft less tail)
\bar{c}	Mean aerodynamic chord
h	c.g. position (fraction of mean chord aft of wing l.e.)
h_n	Neutral point of aircraft (fraction of mean chord aft of wing l.e.)
h_u	Position of main gear (fraction of mean chord aft of wing l.e.)
h_{wb}	Position of aerodynamic centre of wing-body combination (fraction of mean chord aft of wing l.e.)
I_x, I_y, I_z, I_{xz}	Moments of inertia
J	Performance index
\underline{K}	Feedback matrix
\underline{K}_{FR}	Reduced feed forward matrix
\underline{K}_N	Static margin
\underline{K}_p	Precompensator matrix
L_t	Tailplane lift
L_{wb}	Lift of wing-body combination (aircraft less tail)
l_t	Distance between c.g. and tailplane aerodynamic centre
l_t'	Distance between wing and tailplane aerodynamic centres.
M	Pitching moment
M_{wb}	Pitching moment of wing-body combination (aircraft less tail) about c.g.
m	Aircraft mass
\underline{M}	Solution of matrix-Riccati equation
M_w, M_q, M_w	Pitching moment derivatives
n	Number of helicopter blades
p, q, r	Body axis perturbation roll, pitch and yaw rates
$\underline{Q}, \underline{R}$	Weighting matrices of performance index
R	Radius of helicopter rotor blade
S	Wing area
S_T	Tailplane area
\underline{u}	Control vector
u, v, w	Body-axis perturbation velocities
\underline{u}_p	Precompensated control vector
\underline{u}_{pd}	Pilot demanded control vector
\underline{u}^T	Transpose of control vector

V_f	Aircraft velocity along flight path
V_{ftg}	Target velocity along flight path
V_H	Tail volume ratio = $S_{t_l} l_t / S \bar{c}$
V_H'	Tail volume ratio = $S_{t_l} l_t' / S \bar{c}$
\underline{x}	State vector
\underline{x}_R	Reduced state vector
X_u, X_w	Force derivatives along x-axis
x_e, y_e, z_e	Perturbation distances in earth axes
$Z_u, Z_w, Z_q, Z_{\dot{w}}$	Force derivatives along z-axis
α	Angle of attack
α_s	Tailplane setting angle
α_t	Tailplane angle of incidence
γ	Flight path angle
γ_d	Pilot demanded flight path angle
ΔV_f	Perturbation flight speed
ΔV_{fd}	Demanded perturbation flight speed
ϵ	Downwash angle
θ	Pitch attitude deviation angle
θ_d	Pilot demanded pitch attitude deviation angle
θ_e	Trim pitch attitude angle
θ_0	Main rotor collective pitch angle
θ_{1c}	Main rotor lateral cyclic pitch angle
θ_{1s}	Main rotor longitudinal cyclic pitch angle
θ_{otr}	Tail rotor collective pitch angle
ρ	Density of air
ϕ	Roll attitude deviation angle
ψ	Yaw attitude deviation angle
Ω	Rotor speed

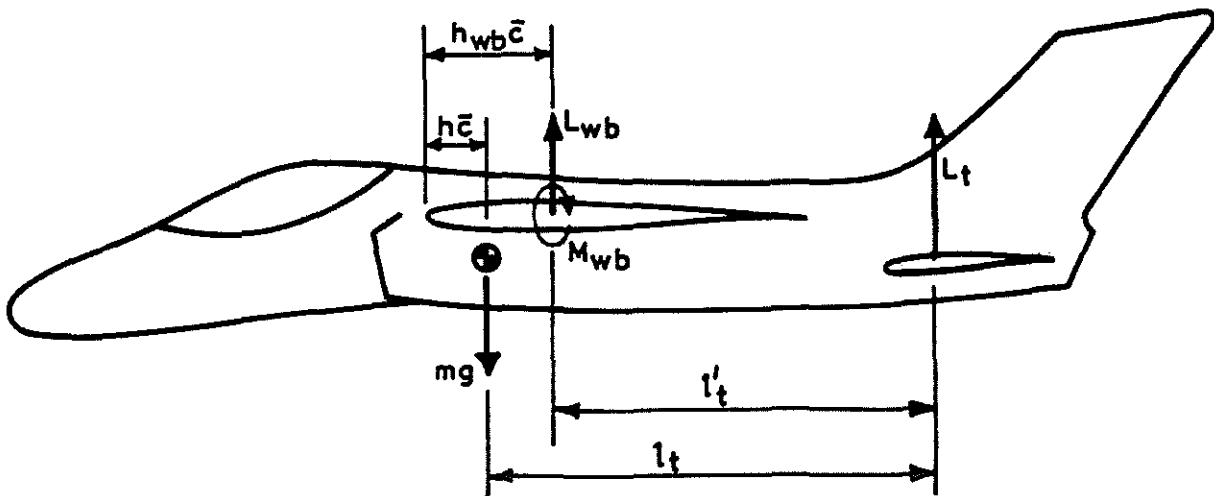


Fig. 1. Straight and level flight

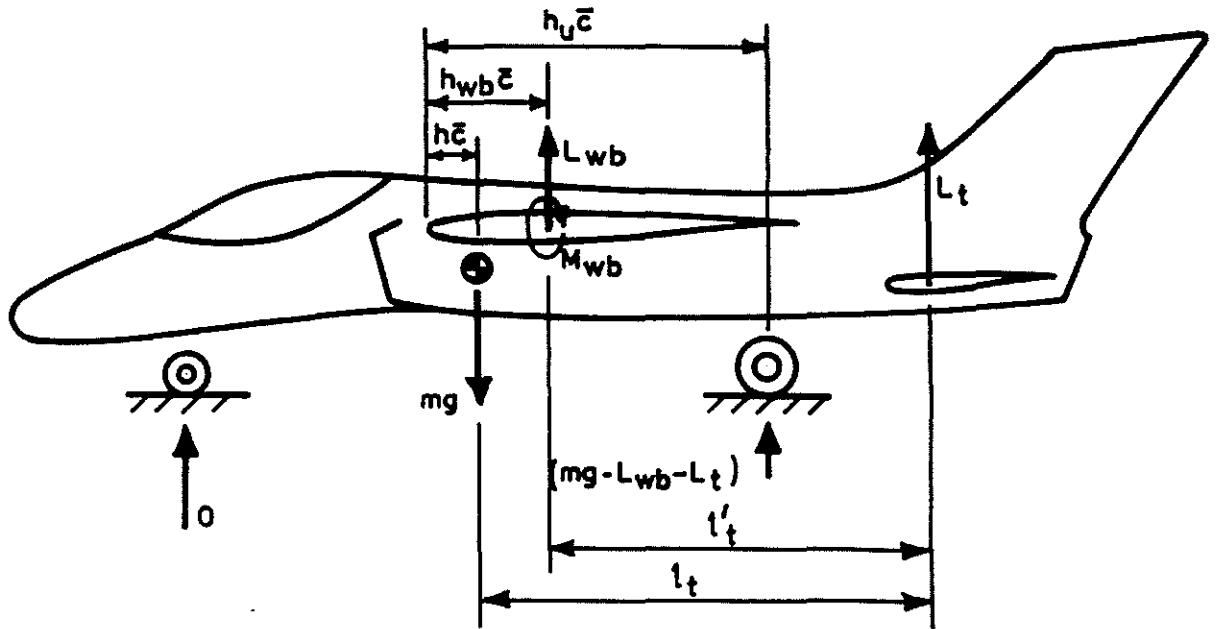


Fig. 2. Rotation at take-off

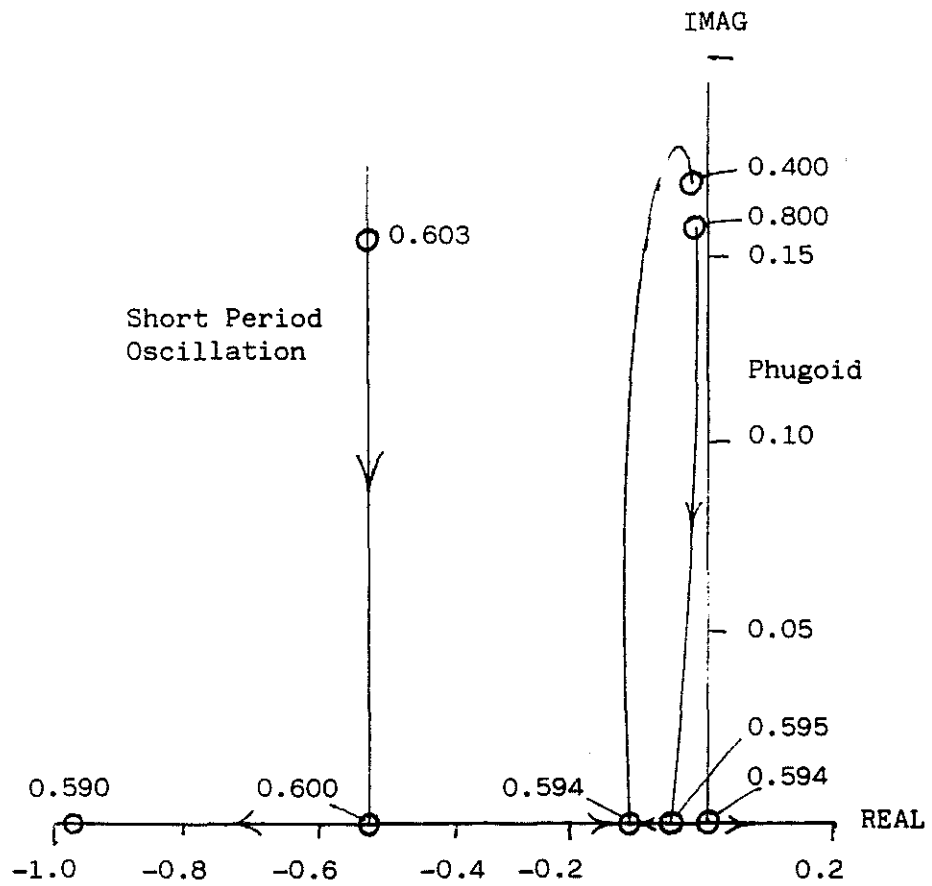


Fig. 3. Effect of decreasing V_{II}' on longitudinal stability of example fixed-wing aircraft

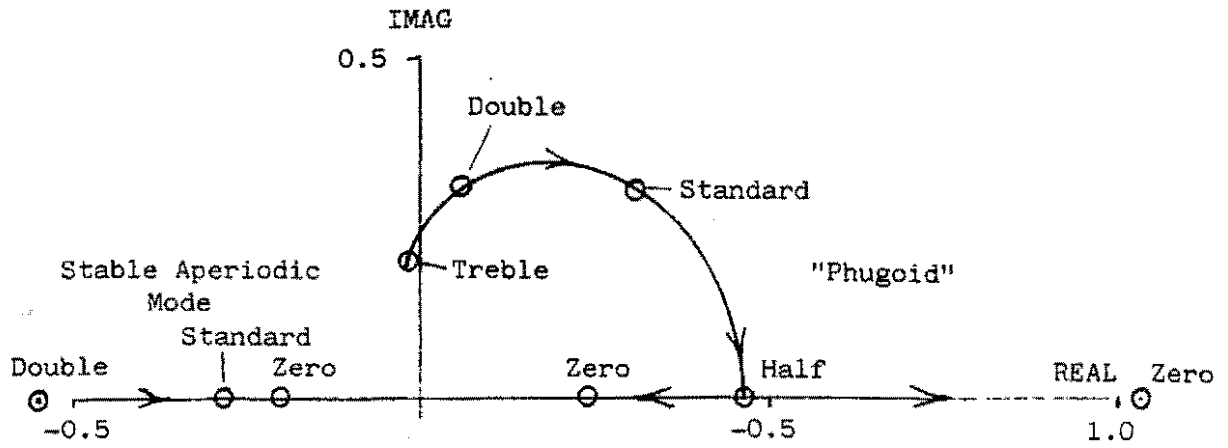


Fig. 4. Effect of tailplane area on longitudinal stability of example rigid rotor helicopter

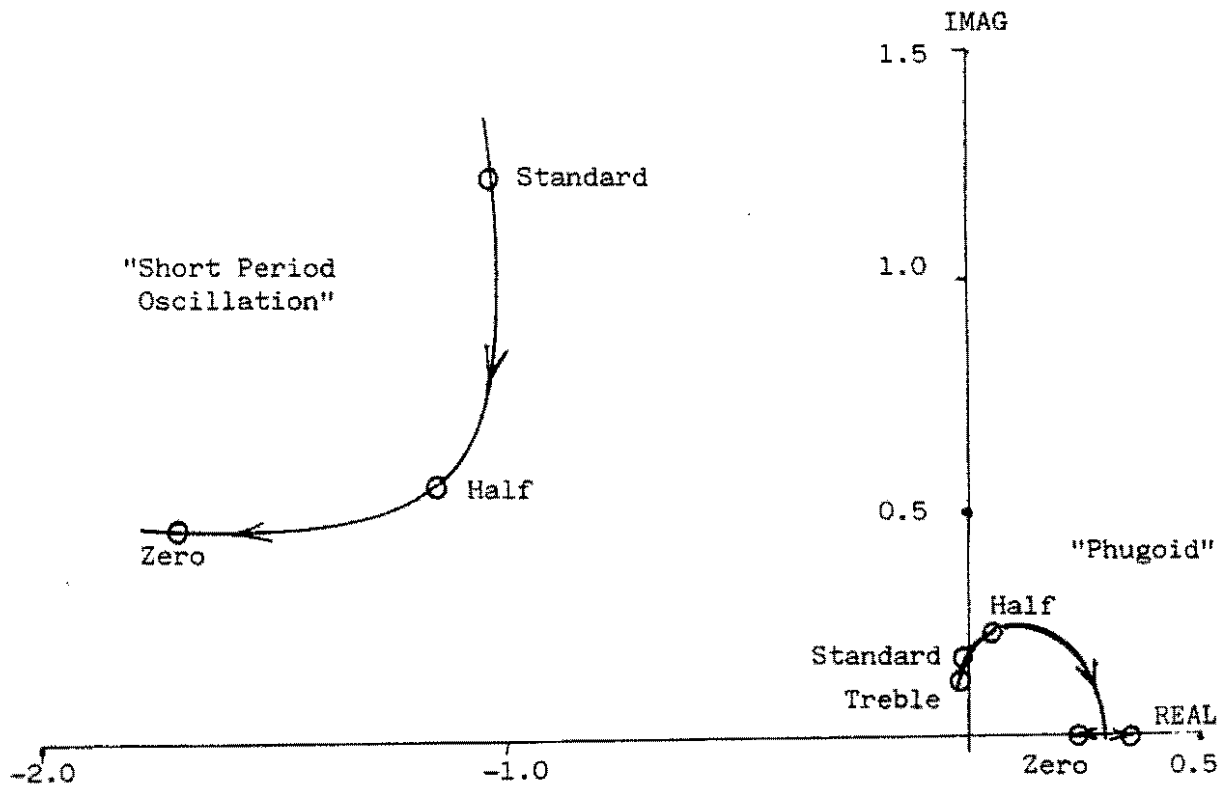


Fig. 5 Effect of tailplane area on longitudinal stability of example articulated rotor helicopter

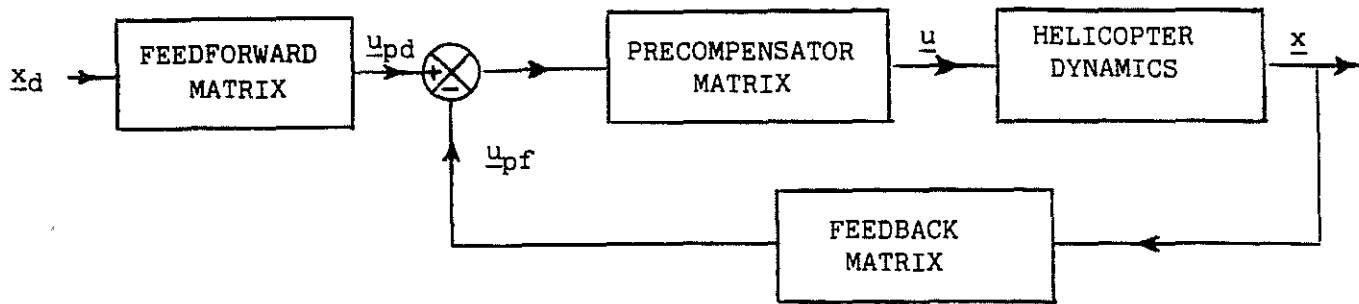


Fig. 6. Block diagram of control system for target tracking manoeuvre

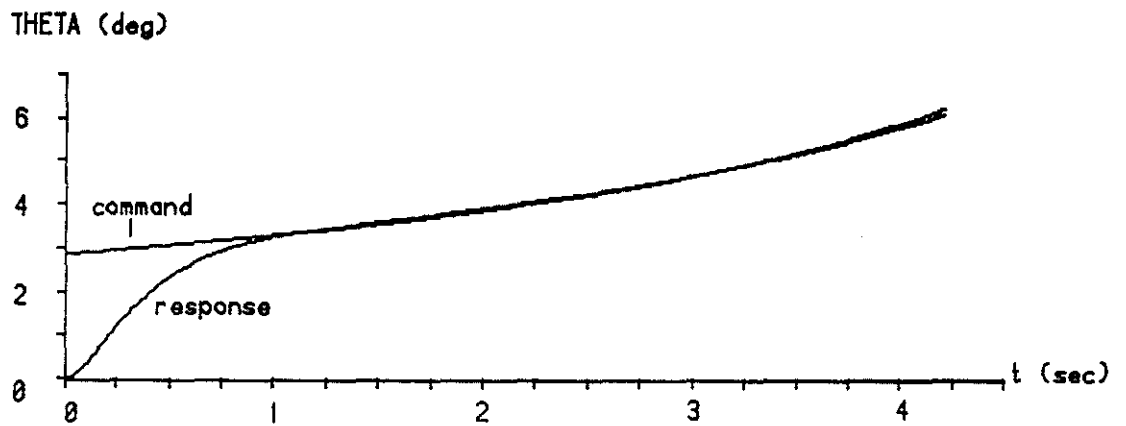


Fig. 7. Pitch attitude deviation during target tracking manoeuvre

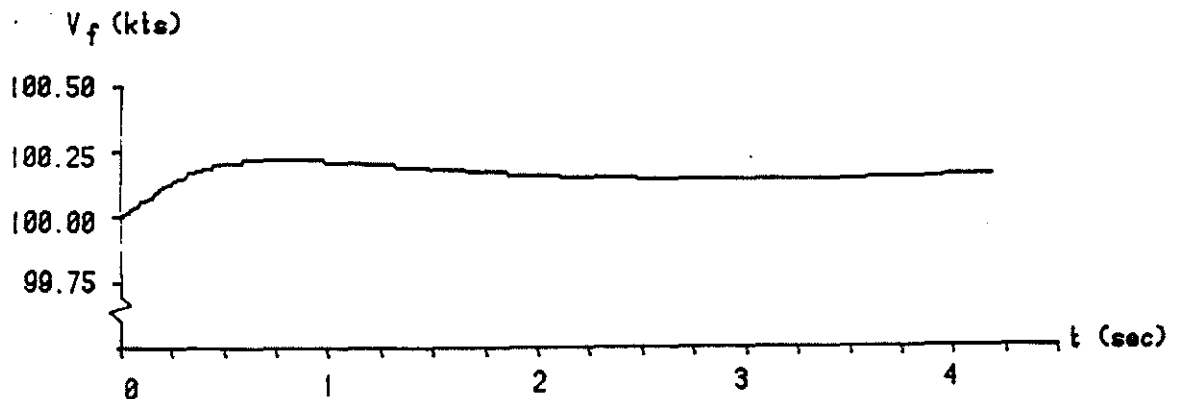


Fig. 8. Speed variation during target tracking manoeuvre

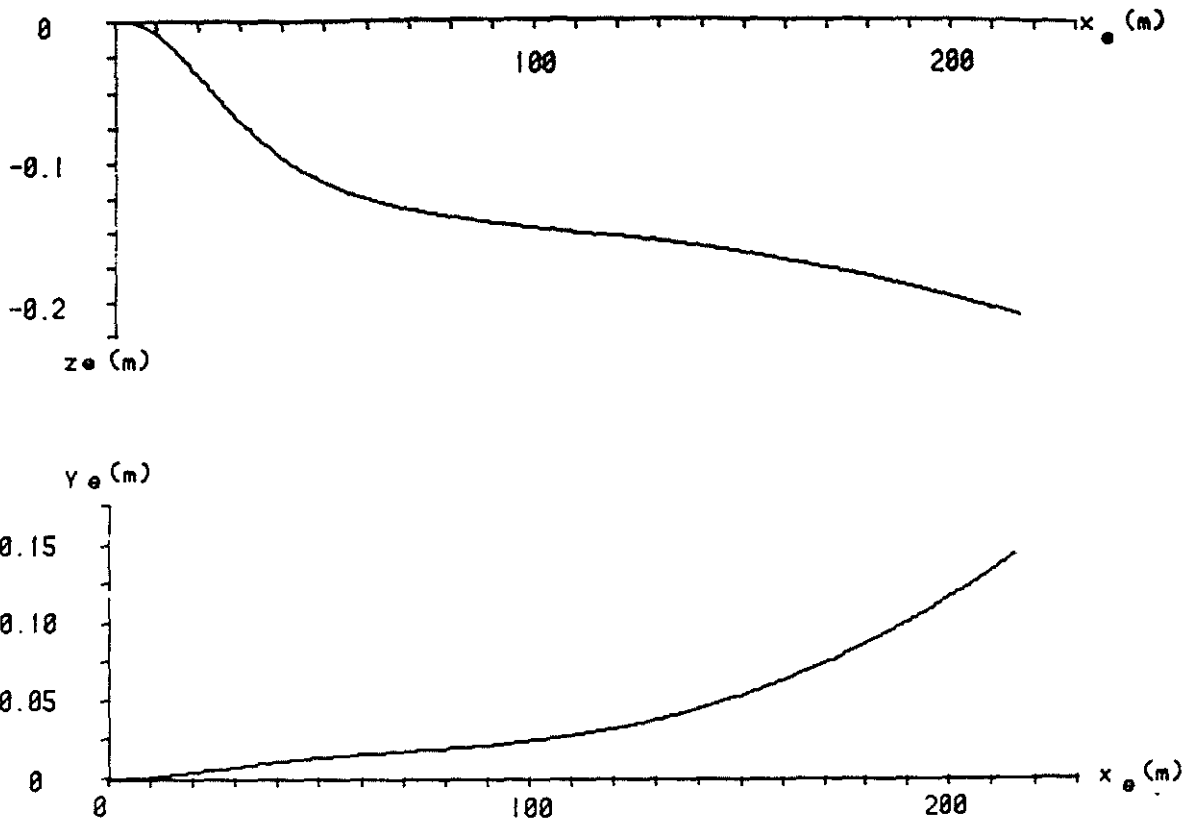


Fig. 9. Flight path during target tracking manoeuvre

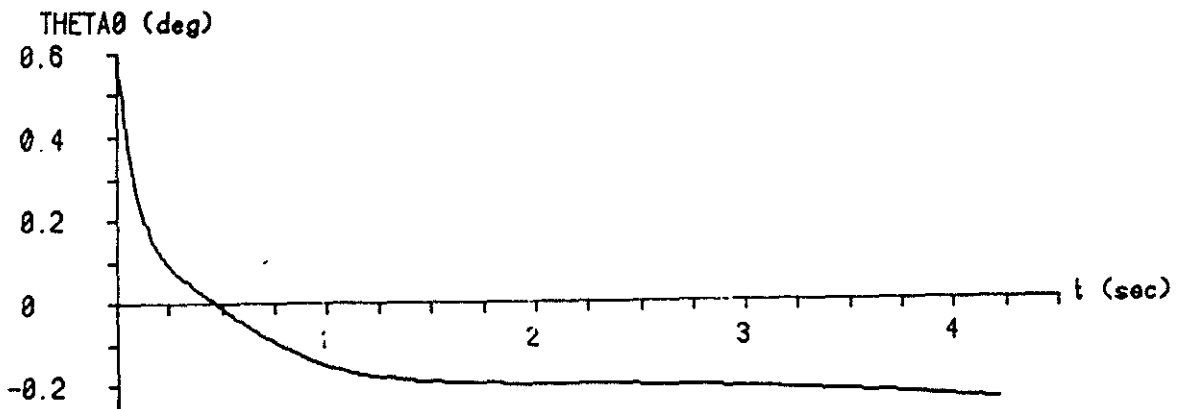


Fig. 10. Control activity during target tracking manoeuvre

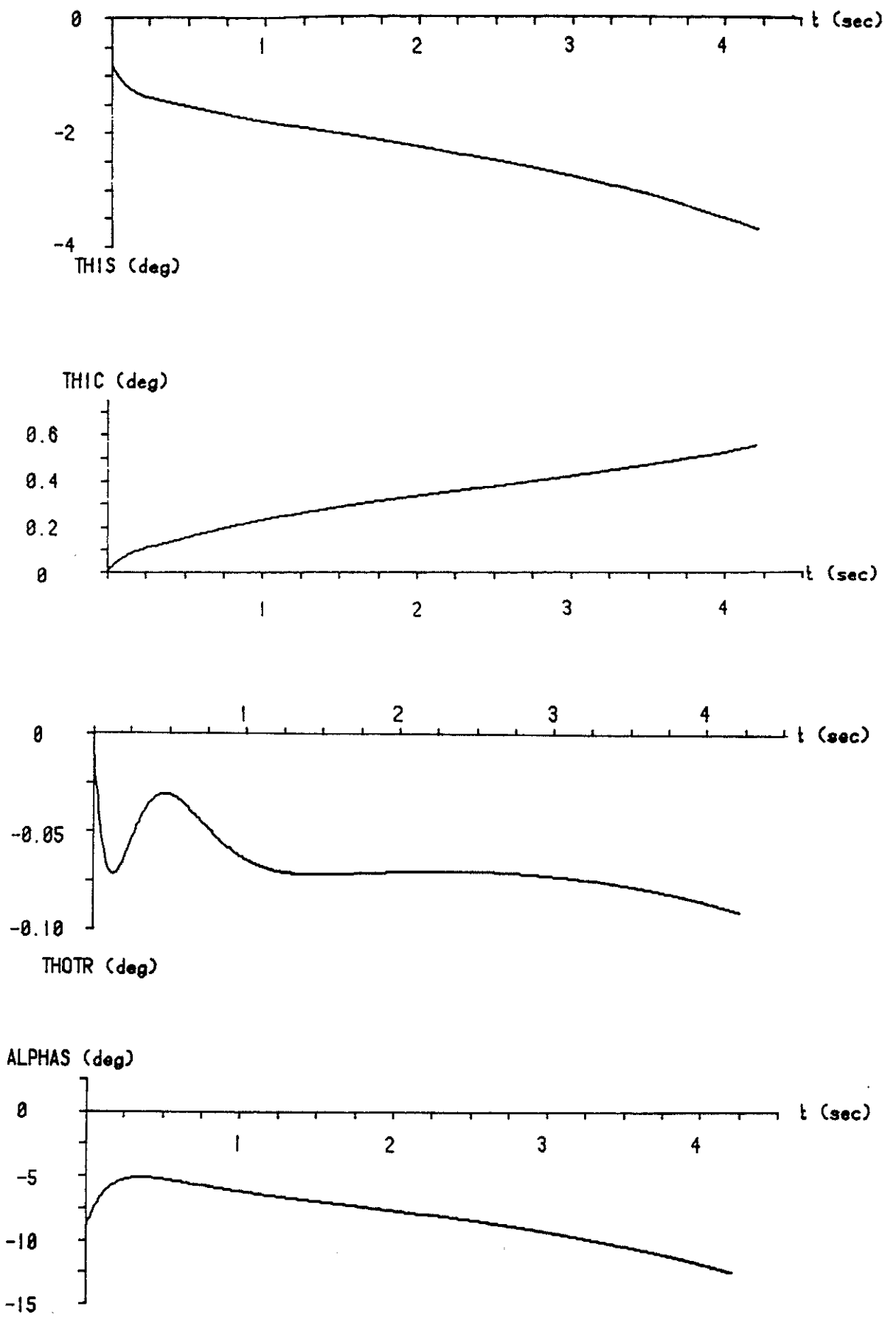


Fig. 10. Control activity during target tracking manoeuvre
(cont'd)

	Aircraft mass m	18000 kg
	Pitching moment of inertia I_y	431235 kgm ²
Wing	Gross area S	52 m ²
	Span	14.8 m
	Mean aerodynamic chord \bar{c}	3.7 m
	Aspect ratio	4.2
	Aerofoil section parallel to line of flight	NACA 65A009
	Thickness/chord ratio	9 %
Tailplane	Design gross area S_t	14.3 m ²
	Lift curve slope a_t	2.92
	Tail moment arm l_t	8.1 m
	Tail volume ratio V_H	0.60
Aerodynamic Derivatives - sea level, $C_L = 0.8$, horizontal flight	$X_u = -352.19$ kg/s	
	$X_w = 932.26$ kg/s	
	$Z_u = -4143.36$ kg/s	
	$Z_w = -9633.31$ kg/s	
	$Z_q = -27978.04 V_H'(0.495 + 0.725 V_H')$ kg-m/s	
	$Z_{\dot{w}} = -215.87 V_H'(0.495 + 0.725 V_H')$ kg	
	$M_w = 40625.64 - 68373.73V_H'$ kg-m/s	
	$M_q = -12053.55$	
	$-237880.40V_H'(0.495 + 0.725V_H')^2$ kg-m ² /s	
	$M_{\dot{w}} = -1823.84 V_H'(0.495 + 0.725 V_H')^2$ kg-m	
Linearised equations of motion	$m\dot{u} - X_u u - X_w w - X_q q - mg\theta = 0$	
	$- Z_u u + (m - Z_{\dot{w}})\dot{w} - Z_w w - (mV + Z_q)q = 0$	
	$- M_{\dot{w}}\dot{w} - M_w w + I_y \dot{q} - M_q q = 0$	
	$q - \theta = 0$	

Table 1 Fixed-Wing Aircraft Data

	Aircraft mass m	4314 kg
	Pitching moment of inertia I_y	13905 kg-m ²
	Yawing moment of inertia I_z	12209 kg-m ²
	Rolling moment of inertia I_x	2767 kg-m ²
	Product of inertia I_{xz}	2035 kg-m ²
Main Rotor	Speed Ω	340 rev/min
	Radius R	6.4 m
	Number of blades n	4
	Solidity	0.078
	Blade lift curve slope	6.00
	Equivalent flapping hinge offset	17%
Tailplane	Design gross area S_t	1.20 m ²
	Tail moment arm l_t	7.66 m
	Lift curve slope a_t	3.50

Table 2 Rigid Rotor Helicopter Data

	Aircraft mass m	5511 kg
	Pitching moment of inertia I_y	32899 kg-m ²
	Yawing moment of inertia I_z	25638 kg-m ²
	Rolling moment of inertia I_x	9659 kg-m ²
	Product of inertia I_{xz}	2022 kg-m ²
Main Rotor	Speed	260 rev/min
	Radius R	7.5 m
	Number of blades n	4
	Solidity	0.092
	Blade lift curve slope	5.73
	Flapping hinge offset	6%
Tailplane	Design gross area S_t	1.34 m ²
	Tail moment arm l_t	9.00 m
	Lift curve slope a_t	3.70

Table 3 Articulated Rotor Helicopter Data

Vehicle	Trim State	Longitudinal Roots
Fixed Wing aircraft (Table 1)	Horizontal flight, sea level, $C_L = 0.8$	-0.5444 ± i 0.6003, -0.0007 ± i 0.1199
Rigid rotor helicopter (Table 2)	Horizontal flight, sea level, 100 knots	-3.8633, -0.2728, 0.3134 ± i 0.3173
Articulated rotor helicopter (Table 3)	Horizontal flight, sea level, 100 knots	-1.0207 ± i 1.2350, -0.0080 ± i 0.1712

Table 4 Longitudinal Stability Characteristics of Standard Configurations

Helicopter	Max Gross Wt. kg	Disc Area m ²	Rotor Solidity	Tailplane Area m ²
Hughes OH-6A	1220	50.593	0.054	0.678
MBB BO-105C	2300	75.738	0.070	0.809
Westland Lynx	4300	128.680	0.078	1.197
Bell AH-1G	4310	141.279	0.065	1.366
Bell UH-1H	4310	168.334	0.046	2.032
Aerospatiale Puma	6700	176.620	0.092	1.339
Sikorsky CH-53D	19050	380.755	0.114	3.710

(Data from refs. 3 and 15)

Table 5 Representative Helicopter Tailplane Sizes

Aircraft	Max. Gross Wt. (kg)	Wing Area (m ²)	Tailplane Area (m ²)
Piper Cheyenne	3946	21.3	3.92
B.Ae. Jetstream 31	6900	25.2	7.80
General Dynamics F-16	10800	27.9	5.92
Shorts 360	11793	42.1	8.49
B.Ae. 125-800	12430	34.8	9.29
Lockheed Hercules	70310	162.1	35.40
Boeing 757	108860	185.3	50.35

(Data from ref. 16)

Table 6 Representative Fixed Wing Aircraft Tailplane Sizes

$$\begin{aligned}
 B &= \begin{bmatrix} -1.0622 & -11.5405 & 1.8698 & 0.0000 & -0.0422 \\ 3.4533 & 0.8109 & -0.0043 & 0.0000 & 0.0548 \\ 6.1944 & 25.6867 & -5.3081 & 0.0000 & -4.0423 \\ 0.0000 & 0.0000 & 0.0000 & 0.0000 & 0.0000 \\ -0.0166 & -2.4179 & -9.8151 & 5.6358 & 0.0000 \\ 13.7373 & -31.3217 & -143.0826 & -1.5270 & 0.0000 \\ 0.0000 & 0.0000 & 0.0000 & 0.0000 & 0.0000 \\ 2.2862 & -5.2127 & -23.8126 & -15.7606 & 0.0000 \\ 0.0000 & 0.0000 & 0.0000 & 0.0000 & 0.0000 \end{bmatrix} \\
 B_p &= \begin{bmatrix} 0.0205 & -11.9189 & 0.1444 & 0.0004 & -0.0470 \\ 3.4375 & 0.0101 & 0.1801 & 0.0258 & 0.0255 \\ -0.0054 & 0.0044 & 0.0009 & 0.0003 & -4.0639 \\ 0.0000 & 0.0000 & 0.0000 & 0.0000 & 0.0000 \\ -0.9320 & 0.0410 & -16.8762 & 5.7304 & 0.0070 \\ 0.0049 & -0.0054 & -145.5923 & -0.0475 & -0.0007 \\ 0.0000 & 0.0000 & 0.0000 & 0.0000 & 0.0000 \\ -0.0138 & 0.0152 & -5.7916 & -15.5144 & 0.0026 \\ 0.0000 & 0.0000 & 0.0000 & 0.0000 & 0.0000 \end{bmatrix}
 \end{aligned}$$

60 knots

Table 7. Effects of precompensator matrix

$$B = \begin{bmatrix} 23.5388 & -1.2204 & 0.7984 & 0.0000 & 1.3132 \\ 1.8629 & 1.0205 & -0.0007 & 0.0000 & 0.1470 \\ 18.5043 & 26.3542 & -5.1119 & 0.0000 & -28.8087 \\ 0.0000 & 0.0000 & 0.0000 & 0.0000 & 0.0000 \\ -0.0568 & -2.0584 & -11.0568 & 9.8528 & 0.0000 \\ 39.3887 & -30.5857 & -145.8775 & -2.6697 & 0.0000 \\ 0.0000 & 0.0000 & 0.0000 & 0.0000 & 0.0000 \\ 6.5553 & -5.0902 & -24.2777 & -27.5538 & 0.0000 \\ 0.0000 & 0.0000 & 0.0000 & 0.0000 & 0.0000 \end{bmatrix}$$

$$B_p = \begin{bmatrix} 24.5390 & -1.3048 & -0.0037 & 0.0257 & 0.0149 \\ 1.8987 & 1.0678 & -0.1105 & -0.0379 & 0.0823 \\ 0.0005 & 0.0064 & -0.0007 & 0.0010 & -28.8124 \\ 0.0000 & 0.0000 & 0.0000 & 0.0000 & 0.0000 \\ -2.9801 & 0.3419 & -17.3790 & 10.0357 & 0.1462 \\ 0.5058 & -0.1002 & -144.0613 & -0.0853 & -0.0199 \\ 0.0000 & 0.0000 & 0.0000 & 0.0000 & 0.0000 \\ -0.0111 & 0.1320 & -6.3904 & -27.1237 & 0.0542 \\ 0.0000 & 0.0000 & 0.0000 & 0.0000 & 0.0000 \end{bmatrix}$$

160 knots

Table 7. Effects of precompensator matrix
(cont'd)

Initial condition	Response time t_0 (sec)	Peak control output
$\Delta V_{f_0} = 5 \text{ms}^{-1}$	$\Delta V_f = 0.05 \Delta V_{f_0}$ at 4.76 s	$\theta_{1s} = 11.82^\circ$
$\gamma_0 = 10^\circ$	$\gamma = 0.05 \gamma_0$ at 0.58 s	$\theta_0 = 11.95^\circ$
$\theta_0 = 10^\circ$	$\theta = 0.05 \theta_0$ at 0.6 s	$\alpha_s = 9.41^\circ$

Table 8. Response to disturbances with optimal feedback control

Initial condition: $\Delta V_{f0} = 5 \text{ms}^{-1}$		
state	peak perturbation	time of peak (sec)
γ	1.033°	0.48
θ	0.179°	0.83
v	0.267 ms^{-1}	0.69
ϕ	-0.089°	1.40
r	-0.299°	0.72

Table 9. Cross-coupling levels with optimal feedback control - forward speed disturbance

Initial condition: $\gamma_0 = 10^\circ$		
state	peak perturbation	time of peak (sec)
ΔV_f	-0.035 ms^{-1}	0.70
θ	0.186°	0.38
v	0.033 ms^{-1}	0.17
ϕ	-0.074°	0.42
r	0.047°	0.55

Table 10. Cross-coupling levels with optimal feedback control - climb angle disturbance

Initial condition: $\theta_0 = 10^\circ$		
state	peak perturbation	time of peak (sec)
ΔV_f	-0.344 ms^{-1}	0.68
γ	0.603°	0.40
v	-0.117 ms^{-1}	0.41
ϕ	1.368°	0.62
r	0.100°	0.47

Table 11. Cross-coupling levels with optimal feedback control - pitch attitude disturbance